SCIENTIFIC REPORTS
nature research

OPEN

A Novel Hybrid Model for Predicting Blast-Induced Ground Vibration Based on k-Nearest Neighbors and Particle Swarm Optimization

Received: 8 March 2019
Accepted: 13 August 2019
Published online: 27 September 2019

Xuan-Nam Bui[1,2], Pirat Jaroonpattanapong[3], Hoang Nguyen[4], Quang-Hieu Tran[1,2] & Nguyen Quoc Long[5]

In this scientific report, a new technique of artificial intelligence which is based on k-nearest neighbors (KNN) and particle swarm optimization (PSO), named as PSO-KNN, was developed and proposed for estimating blast-induced ground vibration (PPV). In the proposed PSO-KNN, the hyper-parameters of the KNN were searched and optimized by the PSO. Accordingly, three forms of kernel function of the KNN were used, Quartic (Q), Tri weight (T), and Cosine (C), which result in three models and abbreviated as PSO-KNN-Q, PSO-KNN-T, and PSO-KNN-C models. The valid of the proposed models was surveyed through comparing with those of benchmarks, random forest (RF), support vector regression (SVR), and an empirical technique. A total of 152 blasting events were recorded and analyzed for this aim. Herein, maximum explosive per blast delay (W) and the distance of PPV measurement (R), were used as the two input parameters for predicting PPV. RMSE, R^2, and MAE were utilized as performance indicators for evaluating the models' accuracy. The outcomes instruct that the PSO algorithm significantly improved the efficiency of the PSO-KNN-Q, PSO-KNN-T, and PSO-KNN-C models. Compared to the three benchmarks models (i.e., RF, SVR, and empirical), the PSO-KNN-T model (RMSE = 0.797, R^2 = 0.977, and MAE = 0.385) performed better; therefore, it can be introduced as a powerful tool, which can be used in practical blasting for reducing unwanted elements induced by PPV in surface mines.

Blasting for rock fragmentation is known as one of the most impressive techniques in the fields of mining and civil engineering. However, it is estimated that only about 20% of the total explosive energy was used for rock fragmentation[1–4]. The remaining of explosive energy is wasted, which cause various undesirable effects to the environment, like, air over-pressure (AOp), flyrock, ground vibration, and back-break[5–7]. Of these effects, ground vibration, that is calculated using peak particle velocity (PPV), is utilized to be the most adverse parameter due to it can cause structural vibration, demolish structures, include instability of bench and slope, and affects the underground water[8–12]. Therefore, precise estimation of blast-produced PPV was needed to decrease its influence on our environment.

Until now, experimental and artificial intelligence (AI) commonly utilized for predicting blast-induced PPV[13]. The first one aims to establish empirical equations based on relationships between explosive charge per blasting delay (W) and the distance of PPV measurement (R)[14–23]. However, these empirical equations provide poor prediction performance in some cases e.g.[24–29]; therefore, the latter is considered.

[1]Department of Surface Mining, Mining Faculty, Hanoi University of Mining and Geology, 18 Vien street, Duc Thang ward, Bac Tu Liem district, Hanoi, Vietnam. [2]Center for Mining, Electro-Mechanical research, Hanoi University of Mining and Geology, 18 Vien street, Duc Thang ward, Bac Tu Liem district, Hanoi, Vietnam. [3]Department of Mining and Petroleum, Chiang Mai University, 239 Huy Kaew rd., M., Chiang Mai, Thailand. [4]Institute of Research and Development, Duy Tan University, Da Nang 550000, Vietnam. [5]Department of Mine Surveying, Hanoi University of Mining and Geology, 18 Vien street, Duc Thang ward, Bac Tu Liem district, Hanoi, Vietnam. Correspondence and requests for materials should be addressed to H.N. (email: nguyenhoang23@duytan.edu.vn)

Literature review shows that AI has proven its various efficient fields with promising performance, especially in advanced engineering as well as in mining and measurement[30–47,48]. In order to estimate blast-induced PPV, Khandelwal and Singh[10] have successfully developed an artificial neural network (ANN) utilizing 154 blasting events at a surface coal mine in India with the conclusion that ANN is a powerful tool to estimate blast-induced PPV. Saadat, *et al.*[27] also explored an ANN model to predict blast-induced PPV of an iron mine in Iran (Gol-E-Gohar) has been reported using 69 blasting events, even a proper result. Using other AI technique (i.e., classification and regression tree – CART), Khandelwal, *et al.*[49] also successfully predicted PPV with high accuracy based on 51 datasets. Based on the advantages of the XGBoost model, Nguyen, *et al.*[50] also investigated and predicted PPV with high performance using 136 datasets (i.e., RMSE = 1.742, $R^2 = 0.952$). In another work, Nguyen, *et al.*[51] optimized the Cubist models by a clustering technique (i.e., hierarchical K-means), for predicting PPV with high reliability. They concluded that the clustering technique can be considered as a robust technique in the classification of the dataset, as well as optimization of the Cubist models. In another work, Hasanipanah, *et al.*[52] utilized the PSO algorithm to predict blast-caused PPV, where two forms, power (P) and linear (L) were used. An empirical technique, along with MLR analysis, are also used for comparing with those of the two PSO models. They reported that the PSO-P provides high prediction performance. Armaghani, *et al.*[53] investigated an integration of PSO with ANN in order to estimate blast-induced PPV, namely PSO-ANN model. They utilized the algorithm of PSO for optimizing the network architecture of the ANN model. A series of empirical equations are additionally applied to estimate PPV and compare with those of the PSO-ANN model. Conclusion of their study is that the PSO-ANN model yielded an outstanding result. In another study, Armaghani, *et al.*[54] used the ICA optimization to estimate blast-induced PPV utilizing 73 blasting events and also a suitable result was determined in their work. Based on the ICA, Hasanipanah, *et al.*[55] also introduced a fuzzy system (FS) model for estimating the model of blast-induced PPV, i.e., FS-ICA. For performing comparisons, a variety of empirical models were also calculated in their study, which proved that the model of FS–ICA outperforms the other experimental approaches. By the use of another optimization algorithm (i.e., firefly algorithm-FFA), Shang, *et al.*[56] developed a new technique to predict PPV using FFA-ANN model. Zhang, *et al.*[57] also developed the PSO-XGBoost technique for the aim of PPV prediction with high performance. In addition, PSO-ANFIS and GA-ANFIS were also investigated by Yang, *et al.*[58], for predicting PPV. Table 1 lists some studies concerning the prediction of blast-induced PPV using AI techniques.

We have found that optimization algorithms are becoming a powerful tool for estimating blast-induced PPV, notably the PSO algorithm. They play a considerable role in the case of enhancing the efficiency of models. However, it was only considered for ANN and XGBoost models. Nevertheless, new hybrid models are needed for knowledge and practical engineering to reduce the undesirable influences of blasting operations. In this work, we expanded the body of knowledge by proposed the PSO optimized *k*-nearest neighbors (KNN) and named as PSO-KNN for estimating blast-induced PPV. The RF, SVR, and empirical models were also considered and exploited to predict PPV based on the same dataset.

Materials

In this study, blasting operations were undertaken at the Deo Nai open-pit coal mine for rock fragmentation. The study site locates in the North of Vietnam, between latitudes 21°01′00″N and 21°20′00″N, and between longitudes 107°18′15″E and 107°19′20″E (Fig. 1). The Arcmap version 10.2 (Link: http://desktop.arcgis.com/en/arcmap/) was used to create the map in Fig. 1. The total area of this mine is ~6.0 km^2 with exploitation reserve of 42.5 Mt, and fertility of 2.5 Mt/yr[59].

The geological structure in the mine is very complicated. Many interleaved faults and folds divide the deposit into many different complex blocks. In this mine, the volume of the overburden is 20 to 30 million m^3/yr. The main bulk of the overburden includes conglomerate, sandstone, siltstone, claystone, and coal clay. Therefore, in this mine, blasting is considered to be imperative for fragmenting rocks. ANFO explosive (ammonium nitrate–fuel oil) was used as the primary explosive in this mine with the hole diameter in the range of 150 to 250 mm. Note that, the non-electric delay blasting method[15,60] is used in this mine in the case of rock breakage.

As stated in the literature[61–63], W and R have the most impacts on PPV, therefore, in this study, both of the W and R parameters are utilized as the primary input parameters for PPV estimation. The Blastmate III perspective (i.e., Instantel in Canada) is utilized for recording the PPV value. Note that the term R was defined by a handheld GPS where W was extracted from 152 blast patterns. Table 2 summaries the data taken in this work. Also, the histograms of each attribute are illustrated in Fig. 2.

Methods

As mentioned above, the principal purpose of this work is to expand a novel hybrid model for estimating blast-induced PPV (i.e., called PSO-KNN model). Moreover, a practical technique and also two algorithms, (e.g., RF and SVR), are also utilized as benchmarks for estimating blast-induced PPV. However, the description of the RF and the SVR has been well documented, i.e., in[64–66]; therefore, the background of the RF and the SVR is not provided in this study.

Empirical. From reviewing the lecture, we have shown that empirical equation of the U.S Bureau of Mines (USBM)[14] is the most common technique where it has been widely applied to estimate PPV produced by blasting operations. Therefore, for the current research, it was implemented for predicting PPV and is demonstrated as:

$$\mathrm{PPV} = \lambda\left(\frac{\mathrm{R}}{\sqrt{\mathrm{W}}}\right)^{-\alpha} \quad (1)$$

References	AI technique
Singh and Singh[8]	ANN
Khandelwal and Singh[61]	ANN
Khandelwal and Singh[9]	ANN
Iphar, *et al.*[107]	ANFIS
Khandelwal and Singh[10]	ANN
Khandelwal, *et al.*[11]	SVM
Monjezi, *et al.*[108]	ANN
Monjezi, *et al.*[24]	ANN
Khandelwal, *et al.*[62]	ANN
Ghasemi, *et al.*[25]	FL
Monjezi, *et al.*[26]	ANN
Saadat, *et al.*[27]	ANN
Armaghani, *et al.*[53]	PSO-ANN
Hasanipanah, *et al.*[109]	SVM
Dindarloo[110]	GA
Hajihassani, *et al.*[28]	ICA-ANN
Hajihassani, *et al.*[111]	PSO-ANN
Amiri, *et al.*[83]	ANN-KNN
Monjezi, *et al.*[112]	GEP
Hasanipanah, *et al.*[113]	CART
Hasanipanah, *et al.*[52]	PSO
Taheri, *et al.*[114]	ABC-ANN
Ragam and Nimaje[115]	GRNN
Armaghani, *et al.*[116]	ICA
Behzadafshar, *et al.*[117]	ICA
Sheykhi, *et al.*[118]	FCM-SVR
Arthur, *et al.*[119]	GP

Table 1. Some studies concerning the prediction of blast-induced PPV using AI techniques. Note: adaptive neuro-fuzzy inference apparatus (ANFIS); support vector machine (SVM); gene expression programming (GEP); fuzzy logic (FL); genetic algorithm (GA); classification and regression tree (CART); artificial bee colony algorithm (ABC); generalized regression neural network (GRNN); fuzzy C-means clustering (FCM); Gaussian process (GP).

Figure 1. Location and landscape of the study site.

W stands for the maximum explosive charge per delay (in Kg);R stands for the monitoring distance (m);where λ and α were the site parameters and were considered using the multivariate regression analysis.

PSO algorithm. In the present work, the algorithm of PSO is utilized for optimizing the KNN model. In the regards of the PSO, more details have been presented in refs.[67–71].

Properties	W	R	PPV
Min.	3200	308.2	2.050
1st Qu.	3952	448.0	8.545
Median	4135	513.0	12.435
Mean	4120	518.3	12.400
3rd Qu.	4295	574.1	15.980
Max.	4643	799.2	29.180

Table 2. Properties of the data taken. Note: W denotes the explosive charge per delay (in Kg); W indicates the monitoring distance (in m); PPV means the intensity of ground vibration (in mm/s).

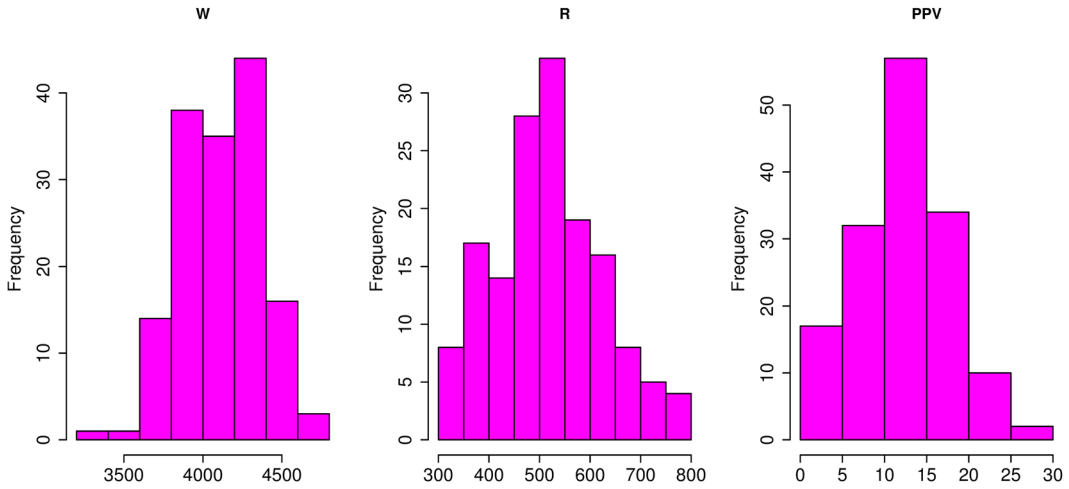

Figure 2. Histogram of the blast-induced ground vibration dataset.

The PSO algorithm is one of the most efficient metaheuristic techniques proposed by Eberhart and Kennedy[72]. This method was adopted from the social animals/particles behavior, like a flock of birds in a swarm and can be used to predict optimization issues with every solution is illustrated as a particle. In order to determine the optimized solution, the algorithm of PSO considers the following steps[73]:

Step 1: Initialize population of particles as well as its related velocity. After that, predict the fitness of particles and discover the best location as local and global best.

Step 2**:** Each particle changes about quest zone with a particular velocity. For each iteration, global best and local best are calculated to assess the efficiency of the PSO-KNN models. Global best is considered as the best-gathered particle position, and the local best is regarded as the best solution in the prevalent iteration.

Step 3: Update the location of a particle**;** After predicting the velocity of particles, the positions of them change about quest zone with the calculated speed and for considered particles, the procedure can calculate and update the new velocity utilizing Eq. 2 as follow:

$$\begin{aligned} v_j^{i+1} &= wv_j^{(i)} + (c_1 \times r_1 \times (local\ best_j - x_j^{(i)})) + (c_2 \times r_2 \times (global\ best_j - x_j^{(i)})),\ v_{\min} \\ &\leq v_j^{(i)} \\ &\leq v_{\max} \end{aligned} \tag{2}$$

where $x_j^{(i)}$ denotes the position of particle j at iteration i; $v_j^{(i)}$ means the particle velocity j for iteration i; w stands for the inertial weight coefficient; i stands for the number of iteration; r_1 and r_2 stand for the numbers in the interval [0,1].

- **The global best and the local best** can be updated when the new particle becomes to remove. The system was calculated and then updated the location, for each particle, using Eq. 3 as below:

$$x_j^{i+1} = x_j^{(i)} + v_j^{(i+1)};\ j = 1, 2, \ldots, n \tag{3}$$

- **Investigate the termination criteria**, when the principle of termination has been satisfied, change the global best as the proper and optimized solution for an issue.

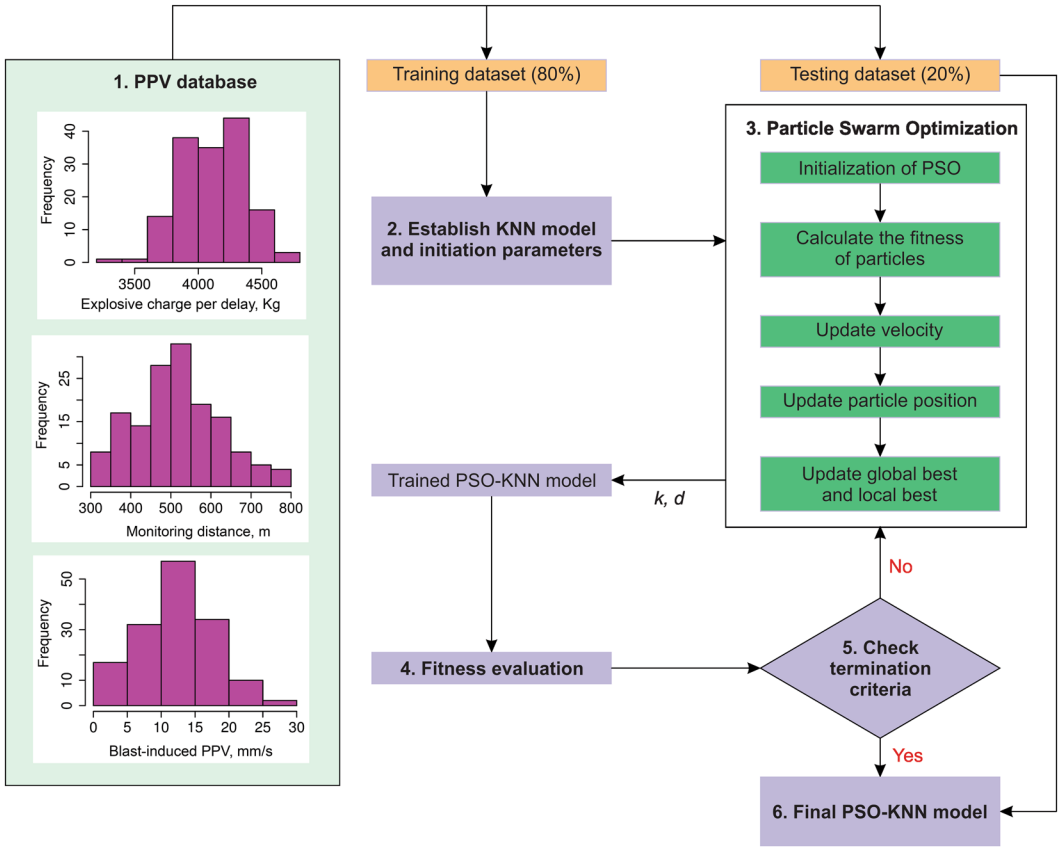

Figure 3. Scheme of a proposed PSO-KNN model for estimating blast-induced PPV.

***k*-Nearest Neighbors (KNN).** The KNN is known as one of the non-parametric approaches in term of classification and regression issues[74]. The most critical parameters of the KNN algorithm are the number of nearest neighbors (k) and the distance metric (d). In regression problems, the parameter k specifies the number of neighbor observations that contribute to the output predictions (i.e., PPV. Instead of considering at the closest reference sample, the algorithm of KNN views at the k instances in the reference collect which is near to the unknown instance as well as performs a vote to make a decision[75,76]. More details in the case of the algorithm of KNN can be obtained in refs.[77–79].

Review of previous works indicate that the KNN algorithms have been applied correctly in many fields[80–82]; however, it seems to be rarely considered for estimating blast-induced problems. Amiri, *et al.*[83] Amiri et al. proposed the model ANN-KNN for the first time. ANN-KNN is composed of two component models of KNN and ANN. Each model predicts test samples, and the obtained outcome is a weighted combination of the findings. Firstly, they use K means clustering to partition the training sample within identical clusters. In order to predict a testing sample by KNN, the nearest teammate instance has been found utilizing the distance of city for the test sample. Then, the values of the factors of the closest train instance were considered to the test instance. For each cluster, besides KNN, an ANN can be trained to utilize the train instance of that cluster. Once the ANN models trained, they can be used to predict PPV on the same group of the testing dataset. However, optimization problems for the ANN model and the KNN approach for estimating blast-induced PPV in their work have not been implemented. The weights and ascending bias, as well as the hidden node of the ANN model, have been reviewed and calculated according to the experimental formulas. Likewise, the KNN model was also determined by the traditional method. Note that, in the present study, the training dataset is not divided by clustering algorithms. The KNN algorithm was applied to develop the KNN model on the whole of the training dataset with the hyper-parameters (k, d) put to use to tune the performance of KNN model. To define the most optimal values for the KNN model, the PSO method was included in the adjustment process of k and d of the KNN model.

Proposing the PSO-KNN model. In the present work, the KNN algorithm is the primary algorithm used to estimate blast-induced PPV. The two main hyper-parameters of the KNN model, including k and d, are utilized to adjust the efficiency of the algorithm. For determining the optimal values of k and d, the PSO algorithm was adopted. As shown in Fig. 3, the particles in PSO performed a global search procedure for the best k and d values of the KNN model, called PSO-KNN model. The expanding of the PSO-KNN algorithm has been accomplished through four steps as:

- Step 1: Making the PPV data and preparing the training and testing databases.

In this step, 152 blasting events were divided into two phases by randomly; 124 blasting activities in the first phase (~ about 80 percent of the whole dataset) are used for the training process to expand the PSO-KNN models. The rest 28 blasting events (~20%) in the second phase were used to check the efficiency of the constructed approaches.

- Step 2: Configuration of the KNN model.

As a criterion, the KNN model is considered as the dominant model to predict PPV in the present work. It is noted that three shapes of kernel function were applied for KNN, including quartic (Q), triweight (T), and cosine (C). These functions are described as following[74,84]:

$$\text{Quartic: } K(u) = \frac{15}{16}(1 - u^2)^2 \tag{4}$$

$$\text{Triweight: } K(u) = \frac{35}{32}(1 - u^2)^3 \tag{5}$$

$$\text{Cosine: } K(u) = \frac{\pi}{4}\cos\left(\frac{\pi}{2}u\right) \tag{6}$$

where K is a function that can be integrated with non-negative real values. The primary purpose of using these kernel functions in the present study is to map the data to a higher dimension with the linear relationship. It makes regression of PPV values more accurate in modeling. More details of kernel functions for the KNN model can be found at the following references[74,84–87].

- Step 3: Optimization of KNN, evaluation of fitness, and check termination criteria.

This step aimed to find an optimal KNN model with the lowest amount of a fitness function by searching the best amounts for the hyper-factors of KNN (k, d) using PSO algorithm. To perform the most appropriate KNN approaches according to the PSO algorithm, RMSE is computed as a fitness function as described in Eq. 7. The flowchart of the suggested PSO-KNN algorithm for estimating blast-induced PPV was illustrated in Fig. 3.

- Step 4: Final PPV predictive model.

After that, the optimization method by the algorithm of PSO is completed, the best hyper-parameters of the KNN model were derived and used to build the final PPV predictive methods. The goodness of the approaches was evaluated via the training dataset and performance statistical indexes like MAE, RMSE, and R^2. The error distribution is provided by RMSE[88,89] illustrating the idea of how proper an approach has adjusted the information via R^2. In an optimal model, the RMSE, and MAE could be equal to zero whenever the R^2 could be equal to 1. The performance indicators are computed as:

$$\text{RMSE} = \sqrt{\frac{1}{n}\sum_{i=1}^{n}(y_{PPVi} - \hat{y}_{PPVi})^2} \tag{7}$$

$$R^2 = 1 - \frac{\sum_i (y_{PPVi} - \hat{y}_{PPVi})^2}{\sum_i (y_{PPVi} - \overline{y})^2} \tag{8}$$

$$\text{MAE} = \frac{1}{n}\sum_{i=1}^{n}|y_{PPVi} - \hat{y}_{PPVi}| \tag{9}$$

n stands for a total number of observations; y_{PPVi} is the measured PPV, $\hat{y}_{PPVi}$ is predicted PPV, and $\overline{y}$ is the mean of y_{PPVi}.

Establishing the Predictive Models

In order to develop PPV predictive models in this work, the database, including 152 blasting events, was split into two parts. According to Nick[90], the most usually utilized train/test ratio was 80:20, which was a proper starting ratio based on Swingler[91,92]; hence, 80% of the total information (around 124 events of blasting) is used as the training database for the first section; the remaining amount that consists of 28 blasting events was recognized as the testing database in the second section.

Empirical model. For the empirical model, λ and α are the site parameters and are found using an analysis of multivariate regression. In the present work, the SPSS method (version 16.0) is employed to specify λ and α according to 124 blasting events of the training database. We found that $\lambda = 0.051$ and $\alpha = -2.596$ are the optimized amounts for the site parameters. In this work, the empirical equation USBM is illustrated as below:

$$\text{PPV} = 0.051\left(\frac{\text{R}}{\sqrt{\text{W}}}\right)^{2.596} \tag{10}$$

RF model. RF is considered as the best decision tree methods suggested by Breiman[93]. It may predict both classification and regression issues, i.e., predict PPV. For this aim, the number of the tree (*ntree*) and randomly

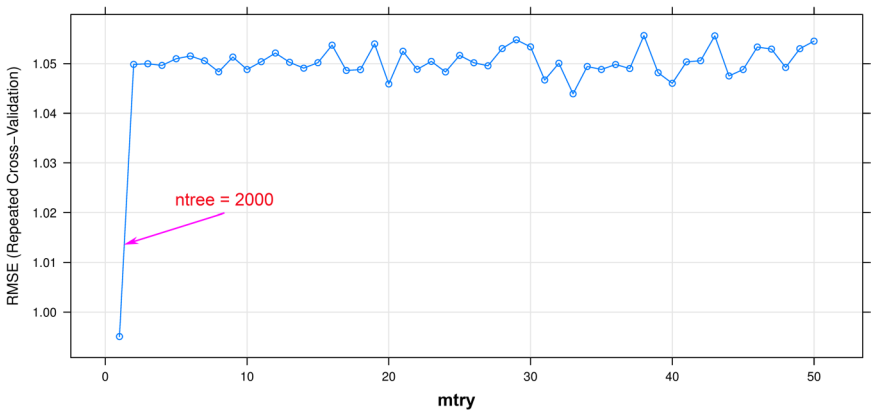

Figure 4. Efficiency of the RF algorithm on the training database.

selected predictor (*mtry*) are the main hyper-parameters involving to adjust the quality of the RF approach. Theoretically, *ntree* must be large enough to avouch the wealth and objectivity of the forest[94]. Each decision tree in the forest acts as a voter. Therefore, *ntree* was set equal to 2000. To introduce the optimized value of the *mtry* parameter, the grid search approach[95] was applied with *mtry* in the range of 1 to 50; The 10-fold cross-validation resampling method[96] is used to avoid over-fitting for RF model. As a result, $ntree = 2000$ and $mtry = 1$ were the best for the RF model (Fig. 4). Its performance was evaluated through RMSE, MAE, and R^2 on the training dataset.

SVR model. For SVR model, the regression problem of PPV was employed through a kernel function. Many previous scientists recommended that the radial basis function (RBF) should be applied in SVR for regression problems with more high accuracy[97–99]. Therefore, the function of the RBF kernel is chosen selected for SVR model with σ and C were the RBF's parameters. The 10-fold cross-validation resampling method is implemented for the SVR model to avoid over-fitting. In the case of expansion of the SVR method, a grid search method for σ and C was established to discover the most proper amounts of the SVR. In this regard, σ was set in the range of 0.1 to around 1; C was adjusted in the range of 50 to 100. Eventually, an optimized SVR method is determined with $\sigma = 0.16$ and $C = 94.5$. Figure 5 indicates the performance of the SVR model for predicting PPV on the training dataset.

PSO-KNN model. In this part, the development of the PSO-KNN method for estimating PPV was presented in detail. As stated earlier, this model is developed via a combination of KNN and PSO algorithms, as shown in Fig. 3. The training dataset for the proposed PSO-KNN method is identical with those utilized in the empirical, RF, and SVR models. According to the training dataset, as the first step, a primary KNN model is produced. Then, as the next step, the hyper-factors of the KNN method are improved using the algorithm of PSO. This part aimed to discover a PPV predictive method with the lowest RMSE by finding the best amounts for the hyperparameters by the algorithm of PSO. In this algorithm, maximum particle's velocity (V_{max}), maximum iteration number (m_i), the population number (p), individual and group cognitive (ϕ_1, ϕ_2), as well as inertia weight (w), are the factors utilized for the optimization approach. The sample size should be large enough to ensure the population diversity[100,101]. Hence, a trial-and-error method is selected, and 50 individuals were the best for the immediate work area ($p = 50$). For the process of terminating the optimization, m_i is adjusted equally to 500[102] for checking the particle positions fitness by utilizing the RMSE metric (Eq. 7). For ensuring the balance among global detection and also local search, w is adjusted equal to around 0.9[103]. Based on previous works, Kennedy[104] and Clerc and Kennedy[105], ϕ_1 can be identical to ϕ_2 and $\phi_1 + \phi_2$ lie in the range of 0 to 4. Hence, in the present work, $\phi_1 = \phi_2 = 1.5$. In order to ensure convergence along with preventing explosion[106], V_{max} is adjusted equal to 2.

Once the PSO's factors are adjusted, the compatibility of particle locations is calculated via the RMSE function. For any definition in the process of optimization, considered particles jump in a constrained checking zone and exchange their experiment to discover the best location (i.e., lowest RMSE); 500 iterations were used to determine the best factors of the suggested PSO-KNN model according to the best position (i.e., lowest RMSE) of the swarm of whole repeats. Note that, three forms of the kernel function (Q, T, C) were applied for the PSO-KNN model as described in the previous section. Figure 6 indicates the efficiency of the optimization approach for the PSO-KNN algorithms. Note that, the best amounts of the hyper-factors obtained for the PSO-KNN models (i.e., after the process of optimization) were determined in Table 3.

Results and Discussions

In the present section, the outcomes of the PPV predictive algorithms were highlighted. The efficiency indexes of the empirical, the RF, the SVR, and the three PSO-KNN models were evaluated based on RMSE, R^2, and MAE, as illustrated in Table 4. The testing database is utilized as the unseen information to check the quality of the expanded models.

Table 4 indicated that the PSO-KNN models properly performed compared to the empirical, RF, and SVR models in estimating PPV. On the training dataset, the PSO-KNN models obtained robust performance with the RMSE in the range of 0.773 to 0.873; R^2 in the range of 0.975 to 0.982; MAE in the field of 0.403 to 0.430. The benchmark models (RF and SVR) were additionally performed quite suitable in this work. But their efficiency

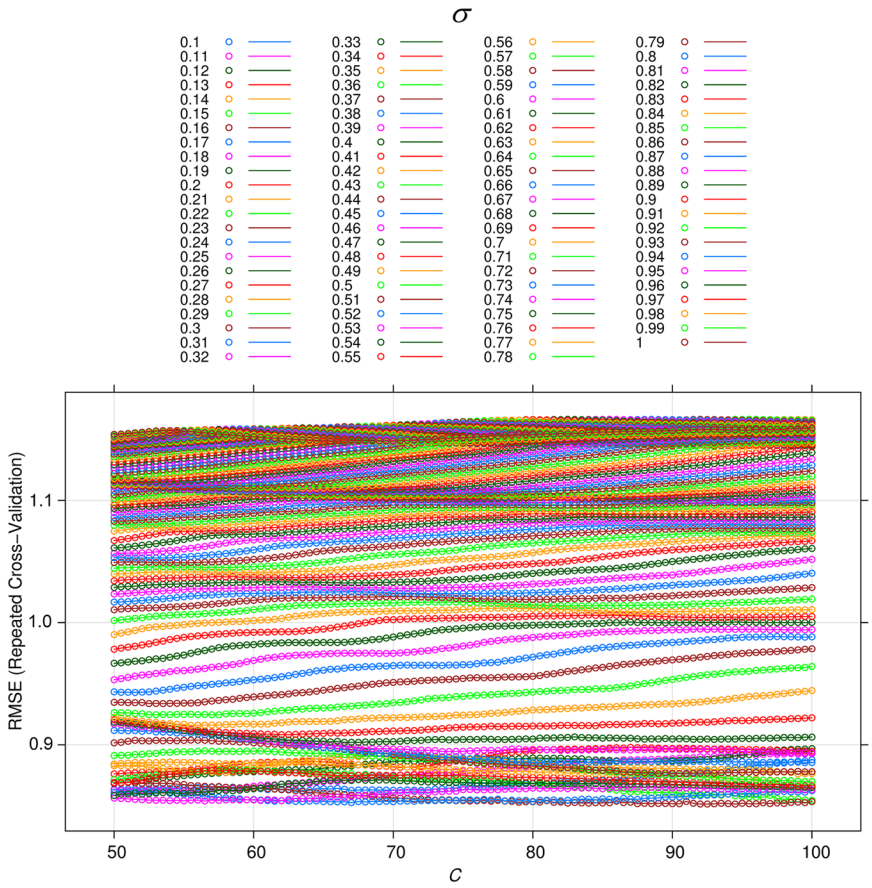

Figure 5. Efficiency of the SVR method on the training dataset.

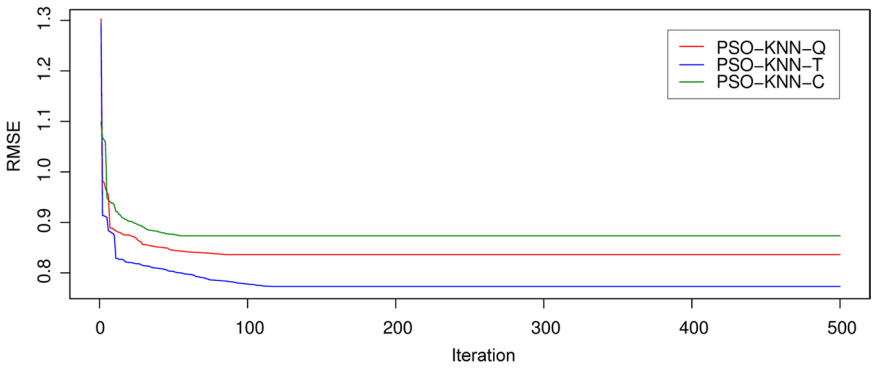

Figure 6. Efficiency of the PSO-KNN models in the process of optimization.

Model	Optimization values of the hyper-parameters	
	k	*d*
PSO-KNN-Q	20	0.493
PSO-KNN-T	10	0.503
PSO-KNN-C	16	0.499

Table 3. The hyper-parameters of PSO-KNN models.

Model	Training dataset			Testing dataset		
	RMSE	R^2	MAE	RMSE	R^2	MAE
Empirical	2.525	0.822	1.306	3.615	0.579	1.727
RF	0.995	0.966	0.508	1.126	0.952	0.499
SVR	0.852	0.973	0.574	1.175	0.944	0.634
PSO-KNN-Q	0.836	0.977	0.417	0.982	0.964	0.454
PSO-KNN-T	**0.773**	**0.982**	**0.403**	**0.797**	**0.977**	**0.385**
PSO-KNN-C	0.873	0.975	0.430	1.014	0.960	0.455

Table 4. Efficiency indexes of the PPV predictive approaches in this work. Note: the best model was shown in bold type.

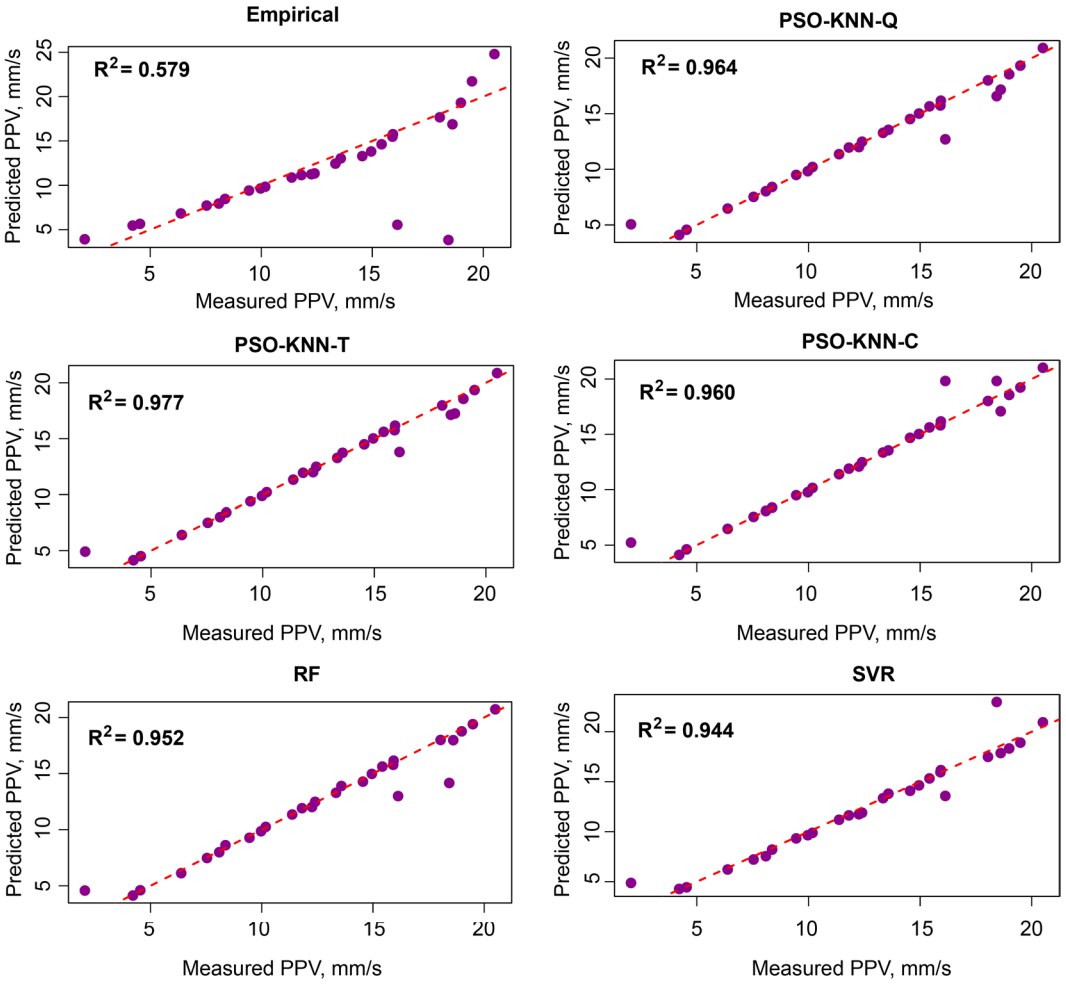

Figure 7. Measured versus predicted values of the models.

was poorer than the PSO-KNN models with an RMSE in the range of 0.852 to 0.995, R^2 in the field of 0.966 to 0.973, and MAE in the range of 0.508 to 0.574. In contrast, the empirical model yielded the poorest performance (RMSE = 2.525, R^2 = 0.822, and MAE = 1.306). Observing the efficiency of the models on the testing dataset, it may be observed that the PSO-KNN algorithms were also outperformed over the other models (RMSE = 0.797 to 1.014; R^2 = 0.960 to 0.977; MAE i = 0.385 to 0.455). Remarkable, the PSO-KNN model with the triweight kernel function (PSO-KNN-T) yielded the most accuracy among the proposed PSO-KNN models (i.e., RMSE = 0.797, R^2 = 0.977, and MAE = 0.385). Next are the PSO-KNN-Q, PSO-KNN-C, RF and SVR models with RNSE in the range of 0.982 to 1.175; R^2 in the range of 0.944 to 0.964; MAE in the range of 0.454 to 0.634. In contrast, the empirical obtained the poorest performance on the testing dataset (i.e., RMSE = 3.615, R^2 = 0.579, and MAE = 1.727). Based on the results in Table 4, all the models are well generalized, especially the PSO-KNN model with triweight kernel function (i.e., PSO-KNN-T) is an outstanding model in term of RMSE, R^2, and MAE. Therefore, it was selected as the most appropriate model for estimating PPV produced by bench blasting. Figure 7

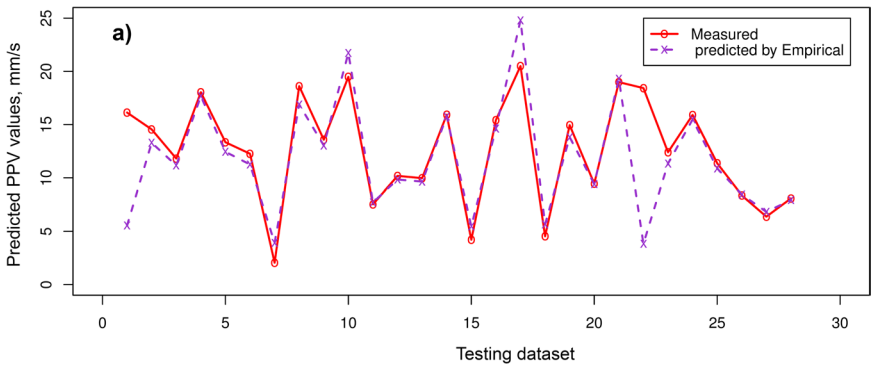

Figure 8. Comparison among exact and estimated amount using the empirical model.

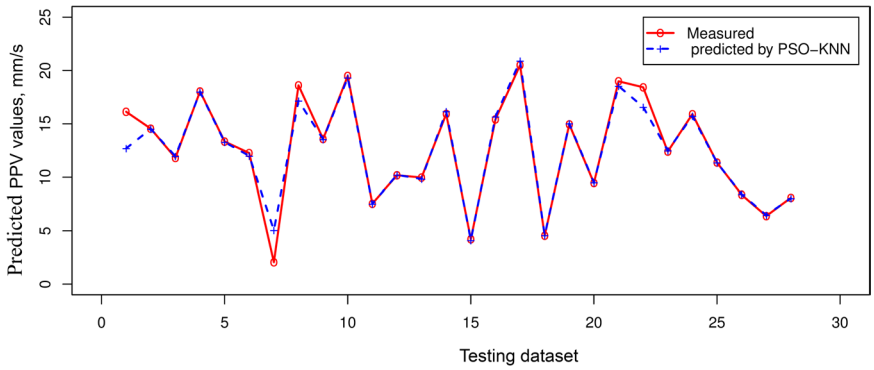

Figure 9. Comparison among exact and estimated amount using the PSO-KNN-T model.

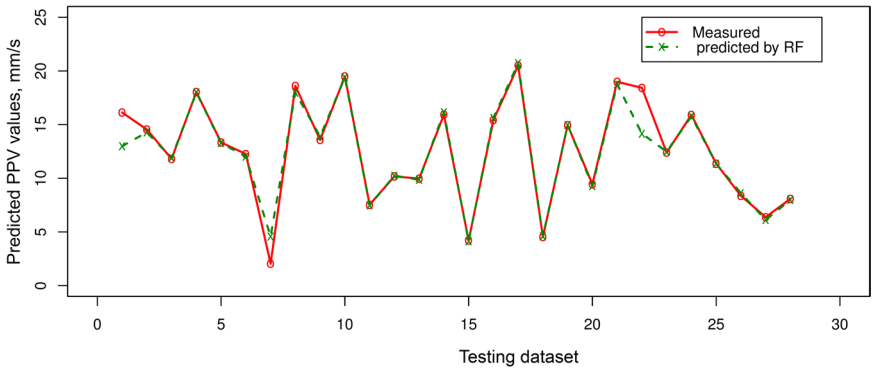

Figure 10. Comparison among exact and estimated amount using the RF model.

shows the efficiency of the models on the testing database. Also, the precision of the expanded models is even compared in Figs 8–11.

Conclusions

Blasting is known as one of the most appropriate and cheapest approaches for the fragmentation of hard-rocks in the case of open-pit mines. Nevertheless, its improper impacts on the surrounding environment, particularly ground vibration (PPV), are unavoidable. Hence, precise blast-induced PPV estimations are essential for decreasing the effects on our environment. The present work proposed a new hybrid technique for estimating PPV according to the KNN and PSO algorithms with high accuracy, namely PSO-KNN. According to the outcomes of this work, authors obtain some results as follows:

- Blast-induced PPV is a usual involved and non-linear issue that is hard to investigate and estimate. High accuracy of the proposed PSO-KNN model in this study indicating that AI techniques are reasonable solutions, which solve this problem better than the empirical method.

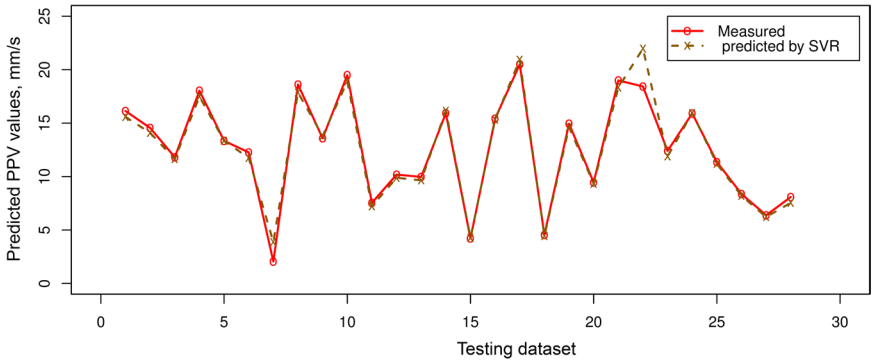

Figure 11. Comparison among exact and estimated amount using the SVR model.

- The PSO algorithm is a suitable optimization tool for estimating purposes of blast-induced PPV. It has a dramatic role in enhancing the precision of the KNN approach, according to RMSE, R^2, and MAE, as illustrated in Table 4. However, the integration of PSO and KNN algorithms are often complexity when setting the parameters.
- The proposed PSO-KNN model (PSO-KNN-T) is a superior approach in estimating PPV induced by bench blasting; therefore, it is an alternative tool that should be considered for other areas in predicting PPV, as well as the other blasting problems in practical engineering.
- This research only considered two parameters of W and R for establishing the blast-induced PPV modes. Therefore, the performance of these models can be enhanced if the other parameters related to the blast pattern and properties of rock mass are to be considered.

Data Availability

All data generated or analyzed during the current study are included.

References

1. Khandelwal, M. & Singh, T. Prediction of blast induced air overpressure in opencast mine. *Noise & Vibration Worldwide* **36**, 7–16 (2005).
2. Verma, A. & Singh, T. Intelligent systems for ground vibration measurement: a comparative study. *Engineering with Computers* **27**, 225–233 (2011).
3. Monjezi, M., Khoshalan, H. A. & Varjani, A. Y. Prediction of flyrock and backbreak in open pit blasting operation: a neuro-genetic approach. *Arabian Journal of Geosciences* **5**, 441–448 (2012).
4. Nguyen, H., Drebenstedt, C., Bui, X.-N. & Bui, D. T. Prediction of Blast-induced Ground Vibration in an Open-pit Mine by a Novel Hybrid Model Based on Clustering and Artificial Neural Network. *Natural Resources Research* (2019).
5. Bui, X. N., Nguyen, H., Le, H. A., Bui, H. B. & Do, N. H. Prediction of Blast-induced Air Over-pressure in Open-Pit Mine: Assessment of Different Artificial Intelligence Techniques. *Natural Resources Research*, https://doi.org/10.1007/s11053-019-09461-0 (2019).
6. Nguyen, H. Support vector regression approach with different kernel functions for predicting blast-induced ground vibration: a case study in an open-pit coal mine of Vietnam. *SN Applied Sciences* **1**, 283, https://doi.org/10.1007/s42452-019-0295-9 (2019).
7. Nguyen, H. *et al*. Evaluating and predicting blast-induced ground vibration in open-cast mine using ANN: a case study in Vietnam. *SN Applied Sciences* **1**, 125, https://doi.org/10.1007/s42452-018-0136-2 (2018).
8. Singh, T. & Singh, V. An intelligent approach to prediction and control ground vibration in mines. *Geotechnical & Geological Engineering* **23**, 249–262 (2005).
9. Khandelwal, M. & Singh, T. Evaluation of blast-induced ground vibration predictors. *Soil Dynamics and Earthquake Engineering* **27**, 116–125 (2007).
10. Khandelwal, M. & Singh, T. Prediction of blast-induced ground vibration using artificial neural network. *International Journal of Rock Mechanics and Mining Sciences* **46**, 1214–1222 (2009).
11. Khandelwal, M., Kankar, P. & Harsha, S. Evaluation and prediction of blast induced ground vibration using support vector machine. *Mining Science and Technology (China)* **20**, 64–70 (2010).
12. Nguyen, H., Bui, X.-N., Tran, Q.-H. & Mai, N.-L. A New Soft Computing Model for Estimating and Controlling Blast-Produced Ground Vibration Based on Hierarchical K-Means Clustering and Cubist Algorithms. *Applied Soft Computing*, 1–20 (2019).
13. Bui, X.-N., Nguyen, H., Le, H.-A., Bui, H.-B. & Do, N.-H. Prediction of Blast-induced Air Over-pressure in Open-Pit Mine: Assessment of Different Artificial Intelligence Techniques. *Natural Resources Research*, 1–25, https://doi.org/10.1007/s11053-019-09461-0 (2019).
14. Duvall, W. I. & Petkof, B. Spherical propagation of explosion-generated strain pulses in rock. (Bureau of Mines, 1958).
15. Langefors, U. & Kihlstrom, B. (JohnWiley and Sons Inc., New York, 1963).
16. Ambraseys, N. Rock Mechanics in Engineering Practice. (1968).
17. Ghosh, A. & Daemen, J. J. In *The 24th US Symposium on Rock Mechanics (USRMS)*. (American Rock Mechanics Association).
18. Roy, P. P. Vibration control in an opencast mine based on improved blast vibration predictors. *Mining Science and Technology* **12**, 157–165 (1991).
19. Hao, H., Wu, Y., Ma, G. & Zhou, Y. Characteristics of surface ground motions induced by blasts in jointed rock mass. *Soil Dynamics and Earthquake Engineering* **21**, 85–98 (2001).
20. Venkatesh, H. Influence of total charge in a blast on the intensity of ground vibrations—field experiment and computer simulation. *Fragblast* **9**, 127–138 (2005).
21. Kuzu, C. The importance of site-specific characters in prediction models for blast-induced ground vibrations. *Soil Dynamics and Earthquake Engineering* **28**, 405–414 (2008).

22. Ak, H. & Konuk, A. The effect of discontinuity frequency on ground vibrations produced from bench blasting: a case study. *Soil Dynamics and Earthquake Engineering* **28**, 686–694 (2008).
23. Simangunsong, G. M. & Wahyudi, S. Effect of bedding plane on prediction blast-induced ground vibration in open pit coal mines. *International Journal of Rock Mechanics and Mining Sciences*, 1–8 (2015).
24. Monjezi, M., Ghafurikalajahi, M. & Bahrami, A. Prediction of blast-induced ground vibration using artificial neural networks. *Tunnelling and Underground Space Technology* **26**, 46–50 (2011).
25. Ghasemi, E., Ataei, M. & Hashemolhosseini, H. Development of a fuzzy model for predicting ground vibration caused by rock blasting in surface mining. *Journal of Vibration and Control* **19**, 755–770 (2013).
26. Monjezi, M., Hasanipanah, M. & Khandelwal, M. Evaluation and prediction of blast-induced ground vibration at Shur River Dam, Iran, by artificial neural network. *Neural Computing and Applications* **22**, 1637–1643 (2013).
27. Saadat, M., Khandelwal, M. & Monjezi, M. An ANN-based approach to predict blast-induced ground vibration of Gol-E-Gohar iron ore mine, Iran. *Journal of Rock Mechanics and Geotechnical Engineering* **6**, 67–76 (2014).
28. Hajihassani, M., Armaghani, D. J., Marto, A. & Mohamad, E. T. Ground vibration prediction in quarry blasting through an artificial neural network optimized by imperialist competitive algorithm. *Bulletin of Engineering Geology and the Environment* **74**, 873–886 (2015).
29. Nguyen, H. & Bui, X.-N. In *Mining sciences and technology - XXVI*. 177–182 (Industry and trade of the socialist republic of Vietnam).
30. Bui, D. T., Nhu, V.-H. & Hoang, N.-D. Prediction of soil compression coefficient for urban housing project using novel integration machine learning approach of swarm intelligence and Multi-layer Perceptron Neural Network. *Advanced Engineering Informatics* **38**, 593–604 (2018).
31. Zhou, Y. & Cao, R. The artificial neural network prediction algorithm research of rail-gun current and armature speed based on B-dot probes array. *Measurement* **133**, 47–55 (2019).
32. Hoang, N.-D. Estimating punching shear capacity of steel fibre reinforced concrete slabs using sequential piecewise multiple linear regression and artificial neural network. *Measurement* **137**, 58–70 (2019).
33. Bilski, P. Data set preprocessing methods for the artificial intelligence-based diagnostic module. *Measurement* **54**, 180–190 (2014).
34. Di Santo, K. G., Di Santo, S. G., Monaro, R. M. & Saidel, M. A. Active demand side management for households in smart grids using optimization and artificial intelligence. *Measurement* **115**, 152–161 (2018).
35. Ponce, H. & Gutiérrez, S. An indoor predicting climate conditions approach using Internet-of-Things and artificial hydrocarbon networks. *Measurement* **135**, 170–179 (2019).
36. Akhani, M., Kashani, A. R., Mousavi, M. & Gandomi, A. H. A hybrid computational intelligence approach to predict spectral acceleration. *Measurement* **138**, 578–589 (2019).
37. Chen, S.-L. & Shu, D.-Y. Measurement forecast of anomalous threshold voltages in BCD LV submicron n-MOSFETs with two artificial intelligence methods. *Measurement* **100**, 93–98 (2017).
38. Chen, T. Forecasting the yield of a semiconductor product using a hybrid-aggregation and entropy-consensus fuzzy collaborative intelligence approach. *Measurement* (2019).
39. Illias, H. A. & Chai, X. R. Hybrid modified evolutionary particle swarm optimisation-time varying acceleration coefficient-artificial neural network for power transformer fault diagnosis. *Measurement* **90**, 94–102 (2016).
40. Koopialipoor, M., Fallah, A., Armaghani, D. J., Azizi, A. & Mohamad, E. T. Three hybrid intelligent models in estimating flyrock distance resulting from blasting. *Engineering with Computers* **35**, 243–256, https://doi.org/10.1007/s00366-018-0596-4 (2019).
41. Armaghani, D. J. *et al*. Evaluation and prediction of flyrock resulting from blasting operations using empirical and computational methods. *Engineering with Computers* **32**, 109–121 (2016).
42. Mohamad, E. T., Armaghani, D. J., Hasanipanah, M., Murlidhar, B. R. & Alel, M. N. A. Estimation of air-overpressure produced by blasting operation through a neuro-genetic technique. *Environmental Earth Sciences* **75**, 174 (2016).
43. Moayedi, H. & Armaghani, D. J. Optimizing an ANN model with ICA for estimating bearing capacity of driven pile in cohesionless soil. *Engineering with Computers* **34**, 347–356 (2018).
44. Moayedi, H. & Hayati, S. Modelling and optimization of ultimate bearing capacity of strip footing near a slope by soft computing methods. *Applied Soft Computing* **66**, 208–219 (2018).
45. Moayedi, H. & Hayati, S. Applicability of a CPT-Based Neural Network Solution in Predicting Load-Settlement Responses of Bored Pile. *International Journal of Geomechanics* **18**, 06018009 (2018).
46. Moayedi, H. & Hayati, S. Artificial intelligence design charts for predicting friction capacity of driven pile in clay. *Neural Computing and Applications*, https://doi.org/10.1007/s00521-018-3555-5 (2018).
47. Moayedi, H. *et al*. Prediction of ultimate bearing capacity through various novel evolutionary and neural network models. *Engineering with Computers*, https://doi.org/10.1007/s00366-019-00723-2 (2019).
48. Panagiotis G. Asteris, Konstantinos G. Kolovos, (2019) Self-compacting concrete strength prediction using surrogate models. Neural Computing and Applications 31 (S1):409-424
49. Khandelwal, M. *et al*. Classification and regression tree technique in estimating peak particle velocity caused by blasting. *Engineering with Computers* **33**, 45–53, https://doi.org/10.1007/s00366-016-0455-0 (2017).
50. Nguyen, H., Bui, X.-N., Bui, H.-B. & Cuong, D. T. Developing an XGBoost model to predict blast-induced peak particle velocity in an open-pit mine: a case study. *Acta Geophysica* **67**, 477–490, https://doi.org/10.1007/s11600-019-00268-4 (2019).
51. Nguyen, H., Bui, X.-N., Tran, Q.-H. & Mai, N.-L. A new soft computing model for estimating and controlling blast-produced ground vibration based on hierarchical K-means clustering and cubist algorithms. *Applied Soft Computing* **77**, 376–386, https://doi.org/10.1016/j.asoc.2019.01.042 (2019).
52. Hasanipanah, M., Naderi, R., Kashir, J., Noorani, S. A. & Qaleh, A. Z. A. Prediction of blast-produced ground vibration using particle swarm optimization. *Engineering with Computers* **33**, 173–179 (2017).
53. Armaghani, D. J., Hajihassani, M., Mohamad, E. T., Marto, A. & Noorani, S. Blasting-induced flyrock and ground vibration prediction through an expert artificial neural network based on particle swarm optimization. *Arabian Journal of Geosciences* **7**, 5383–5396 (2014).
54. Armaghani, D. J., Hasanipanah, M., Amnieh, H. B. & Mohamad, E. T. Feasibility of ICA in approximating ground vibration resulting from mine blasting. *Neural Computing and Applications* **29**, 457–465 (2018).
55. Hasanipanah, M. *et al*. Prediction of an environmental issue of mine blasting: an imperialistic competitive algorithm-based fuzzy system. *International Journal of Environmental Science and Technology* **15**, 551–560 (2018).
56. Shang, Y., Nguyen, H., Bui, X.-N., Tran, Q.-H. & Moayedi, H. A Novel Artificial Intelligence Approach to Predict Blast-Induced Ground Vibration in Open-Pit Mines Based on the Firefly Algorithm and Artificial Neural Network. *Natural Resources Research*, https://doi.org/10.1007/s11053-019-09503-7 (2019).
57. Zhang, X. *et al*. Novel Soft Computing Model for Predicting Blast-Induced Ground Vibration in Open-Pit Mines Based on Particle Swarm Optimization and XGBoost. *Natural Resources Research*, https://doi.org/10.1007/s11053-019-09492-7 (2019).
58. Yang, H., Hasanipanah, M., Tahir, M. M. & Bui, D. T. Intelligent Prediction of Blasting-Induced Ground Vibration Using ANFIS Optimized by GA and PSO. *Natural Resources Research*, https://doi.org/10.1007/s11053-019-09515-3 (2019).
59. Vinacomin. Report on geological exploration of Coc Sau open pit coal mine, Quang Ninh, Vietnam (in Vietnamse-unpublished). (VINACOMIN, Vietnam, 2015).
60. Davitt, A. L. & Simon, J. R. (Google Patents, 1983).

61. Khandelwal, M. & Singh, T. Prediction of blast induced ground vibrations and frequency in opencast mine: a neural network approach. *Journal of sound and vibration* **289**, 711–725 (2006).
62. Khandelwal, M., Kumar, D. L. & Yellishetty, M. Application of soft computing to predict blast-induced ground vibration. *Engineering with Computers* **27**, 117–125 (2011).
63. Nguyen, H., Bui, X.-N., Bui, H.-B. & Cuong, D. T. Developing an XGBoost model to predict blast-induced peak particle velocity in an open-pit mine: a case study. *Acta Geophysica*, 1–14, https://doi.org/10.1007/s11600-019-00268-4 (2019).
64. Drucker, H., Burges, C. J., Kaufman, L., Smola, A. J. & Vapnik, V. *In Advances in neural information processing systems*. 155–161.
65. Liaw, A. & Wiener, M. Classification and regression by randomForest. *R news* **2**, 18–22 (2002).
66. Gao, W., Guirao, J. L., Basavanagoud, B. & Wu, J. Partial multi-dividing ontology learning algorithm. *Information Sciences* **467**, 35–58 (2018).
67. Bansal, J. C. In *Evolutionary and Swarm Intelligence Algorithms* 11–23 (Springer, 2019).
68. Guo, H., Li, H., Xiong, J. & Yu, M. Indoor positioning system based on particle swarm optimization algorithm. *Measurement* **134**, 908–913 (2019).
69. Bensingh, R. J., Machavaram, R., Boopathy, S. R. & Jebaraj, C. Injection molding process optimization of a bi-aspheric lens using hybrid artificial neural networks (ANNs) and particle swarm optimization (PSO). *Measurement* **134**, 359–374 (2019).
70. Nguyen, H. *et al*. Optimizing ANN models with PSO for predicting short building seismic response. *Engineering with Computers*, https://doi.org/10.1007/s00366-019-00733-0 (2019).
71. Nguyen, H., Moayedi, H., Jusoh, W. A. W. & Sharifi, A. Proposing a novel predictive technique using M5Rules-PSO model estimating cooling load in energy-efficient building system. *Engineering with Computers*, https://doi.org/10.1007/s00366-019-00735-y (2019).
72. Eberhart, R. C. & Kennedy, J. In MHS'95. *Proceedings of the Sixth International Symposium on Micro Machine and Human Science*. 39–43 (IEEE).
73. Kennedy, J. In *Encyclopedia of machine learning* 760–766 (Springer, 2011).
74. Altman, N. S. An introduction to kernel and nearest-neighbor nonparametric regression. *The American Statistician* **46**, 175–185 (1992).
75. Yu, K., Ji, L. & Zhang, X. Kernel nearest-neighbor algorithm. *Neural Processing Letters* **15**, 147–156 (2002).
76. Gao, W., Wu, H., Siddiqui, M. K. & Baig, A. Q. Study of biological networks using graph theory. *Saudi journal of biological sciences* **25**, 1212–1219 (2018).
77. Zhou, J., Li, X. & Mitri, H. S. Classification of rockburst in underground projects: Comparison of ten supervised learning methods. *Journal of Computing in Civil Engineering* **30**, 04016003 (2016).
78. Lin, Y., Zhou, K. & Li, J. Application of Cloud Model in Rock Burst Prediction and Performance Comparison with Three Machine Learning Algorithms. *IEEE Access* (2018).
79. Qi, C. & Tang, X. A hybrid ensemble method for improved prediction of slope stability. *International Journal for Numerical and Analytical Methods in Geomechanics* **42**, 1823–1839 (2018).
80. Maillo, J., Ramírez, S., Triguero, I. & Herrera, F. kNN-IS: An Iterative Spark-based design of the k-Nearest Neighbors classifier for big data. *Knowledge-Based Systems* **117**, 3–15 (2017).
81. Ali, L., Kasetkasem, T., Khan, F. G., Chanwimaluang, T. & Nakahara, H. In *Information and Communication Technology for Embedded Systems (IC-ICTES)*, 2017 *8th International Conference of*. 1–6 (IEEE).
82. Wu, X., Yang, J. & Wang, S. Tea category identification based on optimal wavelet entropy and weighted k-Nearest Neighbors algorithm. *Multimedia Tools and Applications* **77**, 3745–3759 (2018).
83. Amiri, M., Amnieh, H. B., Hasanipanah, M. & Khanli, L. M. A new combination of artificial neural network and K-nearest neighbors models to predict blast-induced ground vibration and air-overpressure. *Engineering with Computers* **32**, 631–644 (2016).
84. Cleveland, W. S. & Devlin, S. J. Locally weighted regression: an approach to regression analysis by local fitting. *Journal of the American statistical association* **83**, 596–610 (1988).
85. Epanechnikov, V. A. Non-parametric estimation of a multivariate probability density. *Theory of Probability & Its Applications* **14**, 153–158 (1969).
86. Silverman, B. W. *Density estimation for statistics and data analysis*. (Routledge, 2018).
87. Li, Q. & Racine, J. S. Nonparametric Econometrics: Theory and Practice Princeton University Press (2007).
88. Chai, T. & Draxler, R. R. Root mean square error (RMSE) or mean absolute error (MAE)?–Arguments against avoiding RMSE in the literature. *Geoscientific Model Development* **7**, 1247–1250 (2014).
89. Gao, W., Guirao, J. L. G., Abdel-Aty, M. & Xi, W. An independent set degree condition for fractional critical deleted graphs. *Discrete & Continuous Dynamical Systems-S* (2018).
90. Nick, N. Joseph Juran, 103, Pioneer in Quality Control, Dies. *New York Times* **3**, 3 (2008).
91. Swingler, K. *Applying neural networks: a practical guide*. (Morgan Kaufmann, 1996).
92. Jie Dou, Ali P. Yunus, Dieu Tien Bui, Abdelaziz Merghadi, Mehebub Sahana, Zhongfan Zhu, Chi-Wen Chen, Khabat Khosravi, Yong Yang, Binh Thai Pham, (2019) Assessment of advanced random forest and decision tree algorithms for modeling rainfall-induced landslide susceptibility in the Izu-Oshima Volcanic Island, Japan. Science of The Total Environment 662:332-346
93. Breiman, L. Random forests. *Machine learning* **45**, 5–32 (2001).
94. Nguyen, H. & Bui, X.-N. Predicting Blast-Induced Air Overpressure: A Robust Artificial Intelligence System Based on Artificial Neural Networks and Random Forest. *Natural Resources Research*, https://doi.org/10.1007/s11053-018-9424-1 (2018).
95. Tsirogiannis, G., Perdios, E. & Markellos, V. Improved grid search method: an efficient tool for global computation of periodic orbits. *Celestial Mechanics and Dynamical Astronomy* **103**, 49–78 (2009).
96. Kohavi, R. In *Ijcai*. 1137–1145 (Montreal, Canada).
97. Scholkopf, B. *et al*. Comparing support vector machines with Gaussian kernels to radial basis function classifiers. *IEEE transactions on Signal Processing* **45**, 2758–2765 (1997).
98. Ko, C.-N. & Lee, C.-M. Short-term load forecasting using SVR (support vector regression)-based radial basis function neural network with dual extended Kalman filter. *Energy* **49**, 413–422 (2013).
99. Kisi, O. & Parmar, K. S. Application of least square support vector machine and multivariate adaptive regression spline models in long term prediction of river water pollution. *Journal of Hydrology* **534**, 104–112 (2016).
100. Marinakis, Y., Migdalas, A. & Sifaleras, A. A hybrid particle swarm optimization–variable neighborhood search algorithm for constrained shortest path problems. *European Journal of Operational Research* **261**, 819–834 (2017).
101. Agrawal, A. P. & Kaur, A. In *Data Engineering and Intelligent Computing* 397–405 (Springer, 2018).
102. Bui, D. T. *et al*. Hybrid artificial intelligence approach based on neural fuzzy inference model and metaheuristic optimization for flood susceptibilitgy modeling in a high-frequency tropical cyclone area using GIS. *Journal of Hydrology* **540**, 317–330 (2016).
103. Poli, R., Kennedy, J. & Blackwell, T. Particle swarm optimization. *Swarm intelligence* **1**, 33–57 (2007).
104. Kennedy, J. In *International Conference on Evolutionary Programming*. 579–589 (Springer).
105. Clerc, M. & Kennedy, J. The particle swarm-explosion, stability, and convergence in a multidimensional complex space. *IEEE transactions on Evolutionary Computation* **6**, 58–73 (2002).
106. Eberhart, R. C. & Shi, Y. In *Evolutionary Computation*, 2000. *Proceedings of the 2000 Congress on*. 84–88 (IEEE).
107. Iphar, M., Yavuz, M. & Ak, H. Prediction of ground vibrations resulting from the blasting operations in an open-pit mine by adaptive neuro-fuzzy inference system. *Environmental Geology* **56**, 97–107 (2008).

108. Monjezi, M., Ahmadi, M., Sheikhan, M., Bahrami, A. & Salimi, A. Predicting blast-induced ground vibration using various types of neural networks. *Soil Dynamics and Earthquake Engineering* **30**, 1233–1236 (2010).
109. Hasanipanah, M., Monjezi, M., Shahnazar, A., Armaghani, D. J. & Farazmand, A. Feasibility of indirect determination of blast induced ground vibration based on support vector machine. *Measurement* **75**, 289–297 (2015).
110. Dindarloo, S. R. Prediction of blast-induced ground vibrations via genetic programming. *International Journal of Mining Science and Technology* **25**, 1011–1015 (2015).
111. Hajihassani, M., Armaghani, D. J., Monjezi, M., Mohamad, E. T. & Marto, A. Blast-induced air and ground vibration prediction: a particle swarm optimization-based artificial neural network approach. *Environmental Earth Sciences* **74**, 2799–2817 (2015).
112. Monjezi, M., Baghestani, M., Faradonbeh, R. S., Saghand, M. P. & Armaghani, D. J. Modification and prediction of blast-induced ground vibrations based on both empirical and computational techniques. *Engineering with Computers* **32**, 717–728 (2016).
113. Hasanipanah, M., Faradonbeh, R. S., Amnieh, H. B., Armaghani, D. J. & Monjezi, M. Forecasting blast-induced ground vibration developing a CART model. *Engineering with Computers* **33**, 307–316 (2017).
114. Taheri, K., Hasanipanah, M., Golzar, S. B. & Majid, M. Z. A. A hybrid artificial bee colony algorithm-artificial neural network for forecasting the blast-produced ground vibration. *Engineering with Computers* **33**, 689–700 (2017).
115. Ragam, P. & Nimaje, D. Assessment of blast-induced ground vibration using different predictor approaches-a comparison. *Chemical Engineering Transactions* **66**, 487–492 (2018).
116. Armaghani, D. J., Hasanipanah, M., Amnieh, H. B. & Mohamad, E. T. Feasibility of ICA in approximating ground vibration resulting from mine blasting. *Neural Computing and Applications* **29**, 457–465 (2018).
117. Behzadafshar, K., Mohebbi, F., Soltani Tehrani, M., Hasanipanah, M. & Tabrizi, O. Predicting the ground vibration induced by mine blasting using imperialist competitive algorithm. *Engineering Computations* **35**, 1774–1787 (2018).
118. Sheykhi, H., Bagherpour, R., Ghasemi, E. & Kalhori, H. Forecasting ground vibration due to rock blasting: a hybrid intelligent approach using support vector regression and fuzzy C-means clustering. *Engineering with Computers* **34**, 357–365 (2018).
119. Arthur, C. K., Temeng, V. A. & Ziggah, Y. Y. Novel approach to predicting blast-induced ground vibration using Gaussian process regression. *Engineering with Computers*, 1–14 (2019).

Acknowledgements

This research was supported by Hanoi University of Mining and Geology (HUMG), Hanoi Vietnam; Duy Tan University, Da Nang, Vietnam. We also thank the Center for Mining, Electro-Mechanical research of HUMG for supporting the instruments for data collecting.

Author Contributions

Data collection and experimental works: Xuan-Nam Bui, Quang-Hieu Tran and Nguyen Quoc Long; Writing, discussion, analysis: Xuan-Nam Bui, Pirat Jaroonpattanapong and Hoang Nguyen.

Additional Information

Competing Interests: The authors declare no competing interests.

Publisher's note Springer Nature remains neutral with regard to jurisdictional claims in published maps and institutional affiliations.